


Genome-wide identification of Chiari malformation type I associated candidate genes and chromosomal variations

Timuçin AVŞAR^{1,2,3,*} , Şeyma ÇALIŞ^{3,4} , Baran YILMAZ⁵ , Gülden DEMİRCİ OTLUOĞLU⁵ ,
Can HOLYAVKİN⁴ , Türker KILIÇ^{2,3,5} 

¹Department of Medical Biology, School of Medicine, Bahçeşehir University, İstanbul, Turkey

²Neuroscience Program, Health Sciences Institute, Bahçeşehir University, İstanbul, Turkey

³Neuroscience Laboratory, Health Sciences Institute, Bahçeşehir University, İstanbul, Turkey

⁴Molecular Biology, Genetics, and Biotechnology Graduate Program, Graduate School of Science, Engineering, and Technology, İstanbul Technical University, İstanbul, Turkey

⁵Department of Neurosurgery, School of Medicine, Bahçeşehir University, İstanbul, Turkey

Received: 08.09.2020

Accepted/Published Online: 12.10.2020

Final Version: 14.12.2020

Abstract: Chiari malformation type I (CMI) is a brain malformation that is characterized by herniation of the cerebellum into the spinal canal. Chiari malformation type I is highly heterogeneous; therefore, an accurate explanation of the pathogenesis of the disease is often not possible. Although some studies showed the role of genetics in CMI, the involvement of genetic variations in CMI pathogenesis has not been thoroughly elucidated. Therefore, in the current study we aim to reveal CMI-associated genomic variations in familial cases. Four CMI patients and 7 unaffected healthy members of two distinct families were analyzed. A microarray analysis of the affected and unaffected individuals from two Turkish families with CMI was conducted. Analyses of single nucleotide variations (SNVs) and copy number variations (CNVs) were performed by calculation of B allele frequency (BAF) and log R ratio (LRR) values from whole genome SNV data. Two missense variations, OLFML2A (rs7874348) and SLC4A9 (rs6860077), and a 5'UTR variation of COL4A1 (rs9521687) were significantly associated with CMI. Moreover, 12 SNVs in the intronic regions of FAM155A, NR3C1, TRPC7, ASTN2, and TRAF1 were determined to be associated with CMI. The CNV analysis showed that the 11p15.4 chromosome region is inherited in one of the families. The use of familial studies to explain the molecular pathogenesis of complex diseases such as CMI is crucial. It has been suggested that variations in OLFML2A, SLC4A9, and COL4A1 play a role in CMI molecular pathogenesis. The CNV analysis of individuals in both families revealed a potential chromosomal region, 11p15.4, and risk regions that are associated with CMI.

Key words: Chiari type I malformation, neurogenetics, microarray analysis, molecular karyotyping

1. Introduction

The Chiari malformation (CM) is a condition in which the cerebellar tonsil, which is found at the lower part of the brain right above the foramen magnum, starts extending out through the spinal canal. It blocks spinal fluid flow and can cause fluid accumulation in the canal (syringomyelia) and in the brain. Type I CM (CMI) is the most prevalent type with an incidence rate of approximately 1/1280 (Meadows et al., 2000). Chiari malformation type I can occur due to birth defects and may be detected when the patient is still an infant or during adulthood. However, in some cases—rather than a birth/genetic defect—a traumatic accident or craniocervical tumors may give rise to CMI (Merello et al., 2017). Chiari malformation type I usually comes with accompanying conditions such

as syringomyelia, cerebral hydrocephalus, and basilar invagination (Shah et al., 2017). Almost 70%–80% of CMI cases display syringomyelia (Zhao et al., 2016).

The exact pathogenesis of CMI has yet to be discovered. Currently, CMI is diagnosed in clinic when there are more than 5 mm of tonsils protruding from the foramen magnum (Merello et al., 2017). The broad range of explanations for CMI does not aid in formulating a precise diagnosis. Many other conditions may be included in this type of pathogenesis; therefore, there is a need for more accurate parameters. The most classical proposed mechanism for CMI is a mesodermal defect. Neuroectodermal malformation may also be the cause of CM (Schijman, 2004).

Symptoms vary greatly among CM patients; most of the time these symptoms are as simple as a cough,

* Correspondence: timucin.avsar@med.bau.edu.tr

headache, and nausea. Another diagnostic challenge is that decompression of the foramen magnum is handled through surgery as a way of treating CM. However, over the years risks involving the surgery have been observed; taking genetics into consideration may help in determining whether surgery is suitable (Langridge et al., 2017). Along with MRI diagnosis, genetics can be used in diagnosis. Moreover, genetics will help us to determine the genetic basis of CMI, which may elucidate its natural history or serve as a guide to treatment.

For many years, CM was considered a sporadic disease. However, family studies indicate that genetics are involved in the pathogenesis of CM. Familial aggregation shows that there could be a genetic culprit, and identifying the genes/variants responsible for the pathogenesis may aid in accurate diagnosis and treatment (Nagy et al., 2016; Merello et al., 2017).

Here we present the results of a genome-wide analysis of two Turkish families diagnosed with CMI. We present possible candidate genes associated with familial CMI pathogenesis. Moreover, chromosomal regions and CNVs that are potentially related to CMI are reported.

2. Materials and methods

2.1. Subjects

Two families with individuals diagnosed with CMI are included in the study. Families are labelled with suitable letters. The first family (#MTR) consists of 6 members [2 parents (nonconsanguineous) and 4 children (1 male and 3 female)], and 2 female siblings were operated on for CMI. The second family (#SOY) consists of 5 members [2 parents (nonconsanguineous) and 3 brothers], and the mother and the second son were operated on for CMI. Herniation of the tonsils through the foramen magnum, which causes brain stem pressure, is seen in Figures 1a and 1b (white arrows). Occipital headache during straining or after coughing, dysphagia, numbness in the extremities, and indifference to discrimination between hot/cold sensations, especially in the lower extremities, constituted the main clinical findings.

The other, unaffected members of both families were checked by cranial MRI, and CMI diagnoses were excluded. This study was approved by the institutional review board (2018-17/02). All procedures performed adhered to ethical guidelines. The pedigrees of both

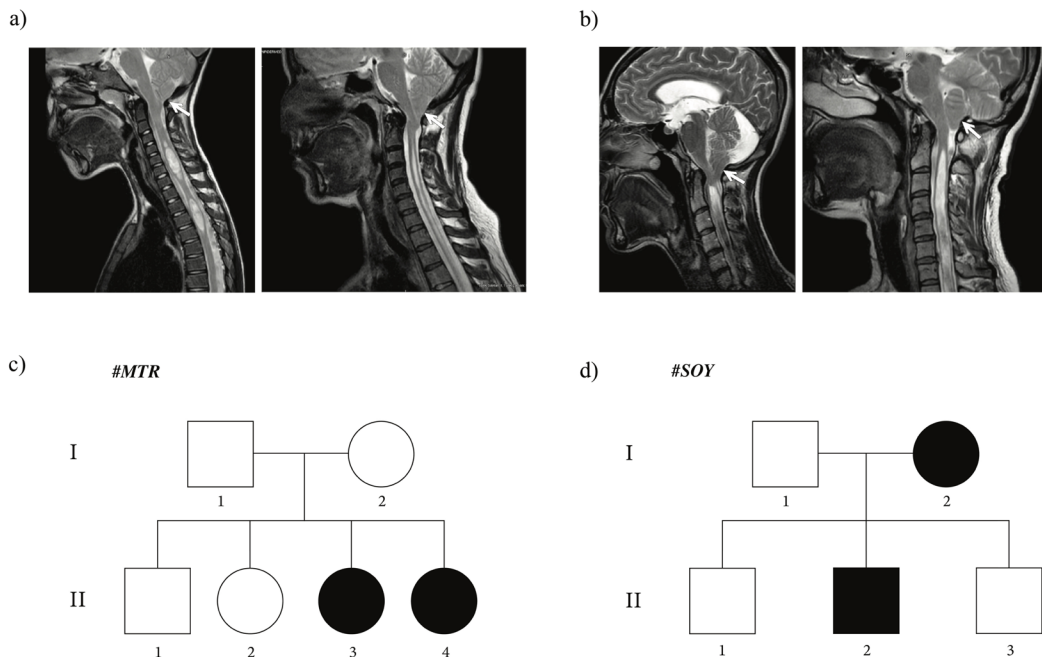


Figure 1. Pedigrees of two Turkish families with CMI. Squares signify males and circles signify females. Filled symbols signify affected individuals. Blood samples of every individual in the pedigrees were collected and subjected to microarray analysis. a) Pedigree of #MTR family. Individuals II-3 daughter and II-4 daughter were confirmed as affected cases. b) MR images of index patients in #MTR family. Left hand side is individual II-3, right hand side is individual II-4. c) Pedigree of #SOY family. Individuals I-2 mother and II-2 son were confirmed as affected cases. d) MR images of index patients in #SOY family. Left hand side is individual I-2, right hand side is individual II-2.

families are shown in Figure 1. In family #MTR, daughters II-3 and II-4 were proband individuals (Figure 1c). Daughter II-3 was operated on when she was 35 years old, and daughter II-4 was operated on when she was 37 years old. Both patients complained of occipital headaches, which were especially aggravated by coughing. In family #SOY, mother (I-2) and son (II-2) were the affected individuals (Figure 1d). The mother (I-2) was 40-years old when she was operated on, and her son (II-2) was 9. The mother's complaint was untreatable headaches and her son's was recurrent falling. The surgical procedure performed in all patients was standardized posterior fossa decompression with additional wide duraplasty.

2.2. Microarray analysis

The isolation of DNA from the blood samples of all individuals in both families shown in the pedigrees (Figure 1) was performed by commercially available kits, according to manufacturer recommendations (NucleoSpin DNA blood, Macherey–Nagel GmbH & Co. KG, Düren, Germany). The DNA samples were studied with an Illumina Infinium CytoSNP-850K v1.2 microarray chip and scanned on Illumina iScan platform (Illumina Inc., San Diego, CA, USA). Around 665,000 single nucleotide polymorphisms (SNPs) were genotyped for each sample. The median range of Illumina microarray chip probes is 2.53 kb. Copy number variation (CNV) analysis was performed by calculation of B allele frequency (BAF) and log R ratio (LRR) values from whole genome SNP data. Copy number variations were determined and visualized via the GenomeStudio (v.2.0.4) and cnvPartition (v.3.2.0) analysis programs provided by Illumina Inc. Human Genome Build 37 was used as a reference to align and report interested positions. The confidence threshold was 50, and GC wave correction was performed for the analysis. In order to determine loss and gain regions, the minimum probe required was set at 8, and copy number loss of heterozygosity (CNLOH) regions greater than 1 Mb were reported.

Microarray results were evaluated by two main approaches. First, SNVs between affected and unaffected members in both families were compared. Mutations in the affected members of both families were reported in Table. Second, chromosomal variations in all affected members and unaffected members were listed for both families in Supplementary Table.

3. Results

3.1. Single nucleotide variations

We evaluated single nucleotide variations (SNVs) in both families and listed those that are common between the two families (Table). Most of these variations were

intronic; however, there were two missense variations and one 5'UTR variation. None of the variations listed in Table were previously reported as clinically significant variations in the ClinVar database (Landrum et al., 2018).

3.2. Copy number variations

Genotype data of microarray results were used to perform copy number variation (CNV) analysis of the affected individuals in both families. Patient II-3 of family MTR harbored no significant CNV, whereas patient II-4 carried 3 copies of 13q13.1 and homozygote deletion of 22q13.2 variations. In family SOY, patient I-2 carried 1 copy of 7q11.21 and 11p15.4, and 3 copies of 11p12 variations, whereas patient II-2 carried 1 copy of 11p15.4 variation. In addition to the CNVs mentioned, all other nonsignificant CNVs that are common in populations and that were detected in the affected individuals of each family were listed in supplementary Table.

4. Discussion

Several previous studies investigated the genetic underpinnings of CMI by using genome wide analyses. One of the most comprehensive studies of CMI included 23 families with 71 affected individuals and microarray data with 10K SNP Chip analysis. Researchers reported a significant linkage on chromosomes 9 and 15 (Boyles et al., 2006). In another comprehensive study, Markunas et al. conducted the largest genome linkage screen in 66 families and 367 individuals. They reported a maximum logarithm of distance (LOD) score of 3 for chromosomes 8 and 12 and listed candidate associated genes such as SUZ12, NF1, and LR6 (Markunas et al., 2013). A similar exploratory analysis of copy number variations in a Turkish family with 2 members affected by CMI failed to identify any significant CNV or gene candidate (Keser et al., 2019). Various studies reported different results. Therefore, we aim to report potential candidate CNVs and genes for familial CMI.

A missense variation was detected in *OLFML2A* gene (rs7874348) (Table). An SNV was found at exon 7 of the gene and caused Thr to Ala amino acid conversion. *OLFML2A* (olfactomedin-like 2A) is an olfactomedin-domain-containing protein, and its function in a cell has not been extensively explored (Sistani et al., 2013). Previous studies state that *OLFML2A* gene has a role in extracellular matrix (ECM) modeling (Furutani et al., 2005; Hong et al., 2019). Since our knowledge about the function of *OLFML2A* gene is limited, we used the STRING database to determine the functional protein association network for our gene of interest (Szkarczyk et al., 2015). Networks shown in Figure 2 demonstrate functional proteins that are connected with *OLFML2A*. Some of the genes shown in the network might be

Table. List of common single nucleotide variations in both families.

Chr. Location	Gene	Biological Process / Gene Ontology ^a	N	Variant ^b	Variant Class ^c	Enhanced Expression ^d
9q33.3	<i>OLFML2A</i>	Protein homodimerization activity	1	rs7874348 (A/G)	Missense	Low tissue specificity
5q31.3	<i>SLC4A9</i>	Anion transmembrane transporter activity	1	rs6860077 (T/C/G)	Missense	Kidney, heart
13q.34	<i>COL4A1</i>	Basal membrane formation	1	rs9521687 (C/A)	5'UTR	Placenta
13q33.3	<i>FAM155A</i>	Calcium ion import across plasma membrane	2	rs1543002 (C/T), rs1543003 (T/A/C)	Intronic	Brain, pituitary gland
5q31.3	<i>NR3C1</i>	Apoptosis, cell cycle, transcription regulation	2	rs4607376 (A/G/T), rs6871464 (T/C)	Intronic	Low Tissue Specificity
5q31.1	<i>TRPC7</i>	Calcium transport	2	rs6893792 (T/A/C), rs10463951 (C/A/G/T)	Intronic	Adrenal gland, brain, intestine, kidney, pituitary gland, testis
9q33.1	<i>ASTN2</i>	Protein transport	5	rs2274414 (T/G), rs16936575 (G/A/T), rs12554069 (T/C), rs6478300 (C/A), rs10983600 (C/T)	Intronic	Low tissue specificity
9q33.2	<i>TRAF1</i>	Apoptosis	1	rs3761847 (G/A)	Intronic	Low tissue specificity
3p24.1	<i>LINC00693</i>	N/A	1	rs9875884 (T/C)	Intronic	Brain
13q33.3	<i>MYO16</i>	Motor activity, actin binding	4	rs76754941 (G/A), rs2759273 (T/C), rs9514937 (G/A), rs9521082 (A/G)	Intronic	Brain
13q.34	<i>COL4A2</i>	Basal membrane formation	7	rs73619284 (C/T), rs8001070 (G/A), rs9555689 (G/A/T), rs7317178 (C/A/T), rs12323265 (A/G), rs9515209 (C/T), rs4517640 (C/T)	Intronic	Placenta
5q31.1	<i>FSTL4</i>	Calcium ion binding, metal ion binding	1	rs55962865 (A/C)	Intronic	Brain
5q31.3	<i>FGF1</i>	Angiogenesis, differentiation	1	rs2339246 (C/G/T)	Intronic	Brain, heart muscle, kidney
5q31.3	<i>ARHGAP26</i>	GTPase activity	1	rs77545201 (G/T)	Intronic	Low tissue specificity
5q32	<i>HTR4</i>	G protein-coupled receptor activity	1	rs1820075 (C/T)	Intronic	Brain, heart muscle, intestine, pituitary gland
5q32	<i>ADRB2</i>	G protein-coupled receptor activity	1	rs6893517 (G/A)	Intronic	Blood
9q32	<i>COL27A1</i>	Extracellular matrix structural constituent	1	rs2567714 (T/C)	Intronic	Brain, uterine, cervix
9q33.1	<i>BRINP1</i>	Inhibits cell proliferation by negative regulation of the G1/S transition	1	rs1332453 (A/C)	Intronic	Brain
9q33.2	<i>PHF19</i>	Chromatin regulator	2	rs11794516 (A/G), rs2072438 (T/C)	Intronic	Low tissue specificity
9q33.2	<i>CNTRL</i>	Cell cycle, cell division	1	rs746182 (T/A/C)	Intronic	Low tissue specificity
9q33.3	<i>MVB12B</i>	Protein transport	1	rs7047946 (G/A)	Intronic	Brain
9q34.11	<i>USP20</i>	Endocytosis, Ubl conjugation pathway	2	rs10819567 (A/C/G), rs62583579 (C/T)	Intronic	Low tissue specificity
9q34.11	<i>LOC101929331</i>	N/A	2	rs10819490 (C/T), rs10988311 (T/G)	Intronic	N/A
5q23.1	<i>LINC00992</i>	N/A	3	rs1863977 (G/A), rs12332110 (G/A/T), rs62380137 (G/A/T)	Intronic	Pancreas, colon

Table. Continued.

5q31.1	LOC100996485	N/A	1	rs2059780 (G/A)	Intronic	N/A
5q31.3	LOC101926941	N/A	3	rs9324876 (A/G), rs959662 (A/C/G), rs9800206 (C/A/T)	Intronic	N/A
17q21.33	LOC100288866	N/A	1	rs2537720 (G/A)	Intronic	Low tissue specificity
7q22.2	LHFPL3	N/A	2	rs2470957 (G/A/T), rs12667640 (T/C)	Intronic	Brain
7q22.3	LHFPL3 - AS2	N/A	1	rs10953457 (C/T)	Intronic	Kidney

N/A: no known function or expression, n: number of reported variations in a gene, ^aAccording to Gene Cards¹ and Gene Ontology² databases, ^bNucleotide changes were determined through dbSNP database³, ^cVariant classes were determined through Genome Browser database⁴, ^dAccording to Gene Cards database.

¹Weizmann Institute of Science (2020). GeneCards: The Human Gene Database [online]. Website <https://www.genecards.org/> [accessed 01 September 2020].

²Gene Ontology Consortium (2020). The Gene Ontology Resource [online]. Website <http://geneontology.org/> [accessed 01 September 2020].

³National Center for Biotechnology Information (2020). dbSNP database [online]. Website <https://www.ncbi.nlm.nih.gov/snp/> [accessed 01 September 2020].

⁴University of California Santa Cruz Genomics Institute (2020). Genome Browser database [online]. Website <https://genome.ucsc.edu> [accessed 01 September 2020].

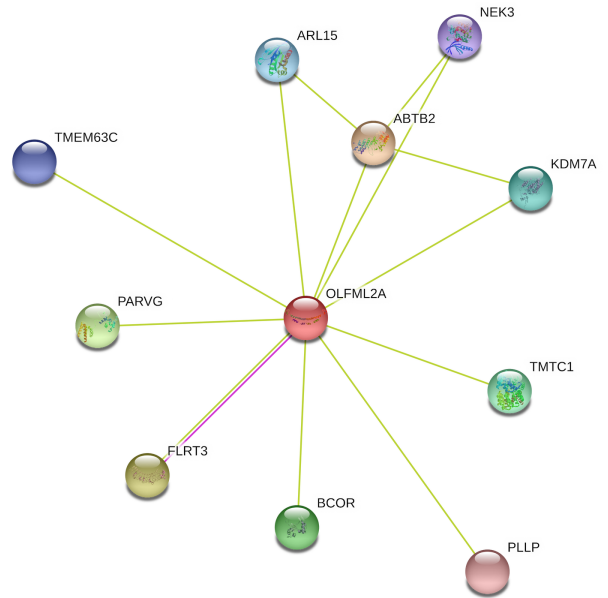


Figure 2. STRING functional protein association network of *OLFML2A* gene (accessed 01 September 2020).

helpful for understanding the cellular processes involving *OLFML2A* (Figure 2). *NEK3* gene encodes for a serine/threonine protein kinase which has a role in neuronal morphogenesis through microtubule acetylation (Chang et al., 2009). *FLRT3* gene was found to be expressed during craniofacial development (Gong et al., 2009), and it functions in cell-cell adhesion and migration during cortical folding (Lu et al., 2015; Del Toro et al., 2017). Lastly, *KDM7A* gene in the network encodes for the histone-demethylase required for brain and craniofacial development (Qi et al., 2010; Tsukada et al., 2010). Hence, we propose that *OLFML2A* gene may be an essential gene in the pathogenesis of CMI due to its role in development of brain structures.

Another missense variation was detected in *SLC4A9* gene (rs6860077) and, similarly, this variation has not been previously reported. It is found at exon 12 of the gene and causes Ile to Met amino acid conversion. Solute carrier family 4 member 9 (*SLC4A9*) belongs to the *SCL4A* family of anion exchangers. Peña-Münzenmayer et al. reported that *SLC4A9* gene has a role in fluid secretion regulation and is specifically responsible for Cl⁻ exchange in the cell (Peña-Münzenmayer et al., 2016). It has been shown that cerebrospinal fluid (CSF) secretion is controlled by Na⁺, Cl⁻, and HCO₃⁻ transportation (Brown et al., 2004). Disrupted CSF flow in the brain may contribute to many pathologies, including CMI, in which the flow is further disrupted due to cerebellar herniation (Buell et al., 2015).

Another significant SNV (rs9521687) was detected in *COL4A1* gene as a 5'UTR variation. This particular SNV has not been associated with any condition, and there are no published studies related to rs9521687. Type IV collagens can only be found in basement membranes, and the family consists of 6 distinct α -chains. The earliest discovered chains, $\alpha 1(IV)$ and $\alpha 2(IV)$, are considered classical chains, and they are encoded by *COL4A1* and *COL4A2*, respectively. Classical chains are expressed both during development and adulthood; however, four other chains are only expressed during development. The $\alpha 1\alpha 1\alpha 2$ triple helix is formed and secreted to the extracellular matrix (ECM), which then becomes a molecular scaffold to other ECM components (Khoshnoodi et al., 2008). Type IV collagen family variations have been associated with various sporadic and genetic diseases. *COL4A1* gene variations may cause poor speech development, cerebral palsy, epilepsy (Pasternak et al., 1980), porencephaly and adult stroke (Gould et al., 2006; van der Knaap et al., 2006), and encephalopathy (Yaramis et al., 2020). These diseases all suggest that *COL4A1* mutations may cause impaired vasculature formation in the brain. Urbizu et al. stated that variations affecting fetal vascular development might cause susceptibility to CMI (Urbizu et al., 2013).

Five of the significantly associated variations (rs1543002, rs10463951, rs4607376, rs6478300, and rs3761847) were reported previously. The SNV (rs1543002) in family with sequence similarity 155 member A gene (*FAM155A*) was reported as a significant SNV for patients diagnosed with bipolar disease and attempted suicide (Willour et al., 2012). Although there is not much information about the function of *FAM155* family genes in humans, studies showed that it is associated with calcium channel activities (Gaudet et al., 2011). Calcium channels are known to have a role in neural tube closure during developmental stages (Abdul-Wajid et al., 2015), and CMI can be classified as an neural tube defect (NTD) in some cases. The SNV (rs4607376) in nuclear receptor subfamily 3 group C member 1 gene (*NR3C1*), which is a glucocorticoid receptor, was previously reported in only one clinical study and it was related with systemic lupus erythematosus (Chen et al., 2017). Although no previous publications have established a relationship between autoimmune diseases and CMI, there have been cases reported suggesting that autoimmune diseases and CM pathogenesis might be related (Ortolani, 2014).

The 3 remaining intronic SNVs (rs10463951) in transient receptor potential cation channel subfamily C member 7 gene (*TRPC7*), (rs6478300) (Wang et al., 2009) in astrotactin 2 gene (*ASTN2*), and (rs3761847) (Huang et al., 2019; Plenge et al., 2007) in TNF receptor associated factor 1 gene (*TRAF1*) are all reportedly related to the autoimmune disease rheumatoid arthritis (RA).

TRPC7 gene is a calcium channel that has a role mainly in keratinocyte development (Beck et al., 2006). *ASTN2* gene encodes for a protein which regulates surface proteins by endocytic trafficking and protein degradation (Behesti et al., 2018). *ASTN2* is reported to form a complex with *ASTN1* which plays a role in neuronal migration, and both genes are highly expressed in the cerebellum (Wilson et al., 2010). *TRAF1* was first identified as a part of the TNFR2 signaling complex, and it also has relationships with other TNFR superfamily members that play a role in prosurvival signaling. *TRAF1* is a well-studied gene, and it has been associated with many different diseases such as B-cell-related cancers, RA, cardiovascular diseases, and many infectious diseases (Edilova et al., 2018).

The CNV analysis provided us with a list of candidate chromosomal regions that are potentially associated with CMI. Furthermore, 11p15.4 one-copy deletion is inherited via mother to son in family SOY.

5. Conclusion

Elucidation of the molecular etiology of CMI by using familial cases is essential for such a complex disease. We conducted molecular karyotyping and SNV analysis for two families and listed important single nucleotide variations with regard to their mutation status and possible roles in CMI etiology. We propose that mutations in *OLFML2A*, *SLC4A9*, and *COL4A1* genes may have a role in the familial form of CMI. Although a number of chromosomal regions were listed as potential regions associated with CMI, only 11p15.4 chromosome regions were CNVs that were inherited by a son via an affected mother. Our explorative results should be confirmed through further familial CMI case studies and molecular studies.

Acknowledgements

We offer our sincere thanks to the Bahçeşehir University Technology Transfer Office (BAU TTO) for the project grant they provided and DONE GENETİK Laboratories for their generous support with their infrastructure.

Disclaimers/conflict of interest

The authors declare no conflict of interest—personal, financial, or institutional— in any of the methods, materials, or devices described in this article. Furthermore, all authors have read and approved the manuscript.

Informed consent

This study was approved by the ethical committee of Bahçeşehir University, School of Medicine (BAU2018-17/02). All patients and family members provided informed consent. All procedures were performed according to the relevant ethical standards.

References

- Abdul-Wajid S, Morales-Diaz H, Khairallah SM, Smith WC (2015). T-type calcium channel regulation of neural tube closure and EphrinA/EPHA expression. *Cell Reports* 13: 829-839.
- Beck B, Zholos A, Sydorenko V, Roudbaraki M, Lehen'kyi V et al. (2006). TRPC7 is a receptor-operated DAG-activated channel in human keratinocytes. *Journal of Investigative Dermatology* 126: 1982-1993.
- Behesti H, Fore TR, Wu P, Horn Z, Leppert M et al. (2018). ASTN2 modulates synaptic strength by trafficking and degradation of surface proteins. *Proceedings of the National Academy of Sciences of the United States of America* 115: E9717-E9726.
- Boyles AL, Enterline DS, Hammock PH, Siegel DG, Slifer SH et al. (2006). Phenotypic definition of Chiari type I malformation coupled with high-density SNP genome screen shows significant evidence for linkage to regions on chromosomes 9 and 15. *American Journal of Medical Genetics Part A* 140: 2776-2785.
- Brown PD, Davies SL, Speake T, Millar ID (2004). Molecular mechanisms of cerebrospinal fluid production. *Neuroscience* 129: 957-970.
- Buell TJ, Heiss JD, Oldfield EH (2015). Pathogenesis and cerebrospinal fluid hydrodynamics of the Chiari I malformation. *Neurosurgery Clinics of North America* 26: 495-499.
- Chang J, Baloh RH, Milbrandt J (2009). The NIMA-family kinase Nek3 regulates microtubule acetylation in neurons. *Journal of Cell Science* 122: 2274-2282.
- Chen JQ, Papp G, Póliska S, Szabó K, Tarr T et al. (2017). MicroRNA expression profiles identify disease-specific alterations in systemic lupus erythematosus and primary Sjögren's syndrome. *PLoS One* 12: e0174585.
- Del Toro D, Ruff T, Cederfjäll E, Villalba A, Seyit-Bremer G et al. (2017). Regulation of cerebral cortex folding by controlling neuronal migration via FLRT adhesion molecules. *Cell* 169: 621-635.e616.
- Edilova MI, Abdul-Sater AA, Watts TH (2018). TRAF1 signaling in human health and disease. *Frontiers in Immunology* 9: 2969-2969.
- Furutani Y, Manabe R-I, Tsutsui K, Yamada T, Sugimoto N et al. (2005). Identification and characterization of photomedins: novel olfactomedin-domain-containing proteins with chondroitin sulphate-E-binding activity. *Biochemical Journal* 389: 675-684.
- Gaudet P, Livstone MS, Lewis SE, Thomas PD (2011). Phylogenetic-based propagation of functional annotations within the Gene Ontology consortium. *Briefings in Bioinformatics* 12: 449-462.
- Gong SG, Mai S, Chung K, Wei K (2009). Flrt2 and Flrt3 have overlapping and non-overlapping expression during craniofacial development. *Gene Expression Patterns* 9: 497-502.
- Gould DB, Phalan FC, Van Mil SE, Sundberg JP, Vahedi K et al. (2006). Role of COL4A1 in small-vessel disease and hemorrhagic stroke. *New England Journal of Medicine* 354: 1489-1496.
- Hong EP, Kim BJ, Cho SS, Yang JS, Choi HJ et al. (2019). Genomic variations in susceptibility to intracranial aneurysm in the Korean population. *Journal of Clinical Medicine* 8: 275.
- Huang S-C, Hua D-J, Sun Q-Q, Zhang L-N, Cen H et al. (2019). Associations of TRAF1/C5 rs10818488 and rs3761847 polymorphisms with genetic susceptibility to rheumatoid arthritis: a case-control study and updated meta-analysis. *Central European Journal of Immunology* 44: 159-173.
- Keser N, Kuskucu A, Is M, Celikoglu E (2019). Familial Chiari type I: a molecular karyotyping study in a Turkish family and review of the literature. *World Neurosurgery* 121: e852-e857.
- Khoshnoodi J, Pedchenko V, Hudson BG (2008). Mammalian collagen IV. *Microscopy Research and Technique* 71: 357-370.
- Landrum MJ, Lee JM, Benson M, Brown GR, Chao C et al. (2018). ClinVar: improving access to variant interpretations and supporting evidence. *Nucleic Acids Research* 46: D1062-D1067.
- Langridge B, Phillips E, Choi D (2017). Chiari malformation type I: a systematic review of natural history and conservative management. *World Neurosurgery* 104: 213-219.
- Lu YC, Nazarko OV, Sando III R, Salzman GS, Li N-S et al. (2015). Structural basis of latrophilin-FLRT-UNC5 interaction in cell adhesion. *Structure* 23: 1678-1691.
- Markunas CA, Soldano K, Dunlap K, Cope H, Asimwe E et al. (2013). Stratified whole genome linkage analysis of Chiari type I malformation implicates known Klippel-Feil syndrome genes as putative disease candidates. *PLoS One* 8: e61521.
- Meadows J, Kraut M, Guarnieri M, Haroun RI, Carson BS (2000). Asymptomatic Chiari type I malformations identified on magnetic resonance imaging. *Journal of Neurosurgery* 92: 920-926.
- Merello E, Tattini L, Magi A, Accogli A, Piatelli G et al. (2017). Exome sequencing of two Italian pedigrees with non-isolated Chiari malformation type I reveals candidate genes for craniofacial development. *European Journal of Human Genetics* 25: 952-959.
- Nagy L, Mobley J, Ray C (2016). Familial aggregation of Chiari malformation: presentation, pedigree, and review of the literature. *Turkish Neurosurgery* 26: 315-320.
- Ortolani F, Tummolo A, Fedele S, Masciopinto M, Pesce S et al. (2014). Autoimmune disease and Arnold Chiari syndrome: any correlation? *Hormone Research in Paediatrics* 82.
- Pasternak JE, Mantovani JE, Volpe JJ (1980). Porencephaly from periventricular intracerebral hemorrhage in a premature infant. *The American Journal of Diseases Children* 134: 673-675.

- Peña-Münzenmayer G, George AT, Shull GE, Melvin JE, Catalán MA (2016). Ae4 (Slc4a9) is an electroneutral monovalent cation-dependent Cl⁻/HCO₃⁻ exchanger. *Journal of General Physiology* 147: 423-436.
- Plenge RM, Seielstad M, Padyukov L, Lee AT, Remmers EF et al. (2007). TRAF1-C5 as a risk locus for rheumatoid arthritis — a genomewide study. *New England Journal of Medicine* 357: 1199-1209.
- Qi HH, Sarkissian M, Hu GQ, Wang Z, Bhattacharjee A et al. (2010). Histone H4K20/H3K9 demethylase PHF8 regulates zebrafish brain and craniofacial development. *Nature* 466: 503-507.
- Schijman E (2004). History, anatomic forms, and pathogenesis of Chiari I malformations. *Child's Nervous System* 20: 323-328.
- Shah A, Dhar A, Elsanafiry M, Goel A (2017). Chiari malformation: has the dilemma ended? *Journal of Craniovertebral Junction and Spine* 8: 297-304.
- Sistani L, Rodriguez PQ, Hulthenby K, Uhlen M, Betsholtz C et al. (2013). Neuronal proteins are novel components of podocyte major processes and their expression in glomerular crescents supports their role in crescent formation. *Kidney International* 83: 63-71.
- Szklarczyk D, Franceschini A, Wyder S, Forslund K, Heller D et al. (2015). STRING v10: protein-protein interaction networks, integrated over the tree of life. *Nucleic Acids Research* 43: D447-D452.
- Tsukada Y-i, Ishitani T, Nakayama KI (2010). KDM7 is a dual demethylase for histone H3 Lys 9 and Lys 27 and functions in brain development. *Genes and Development* 24: 432-437.
- Urbizu A, Toma C, Poca MA, Sahuquillo J, Cuenca-León E et al. (2013). Chiari malformation type I: a case-control association study of 58 developmental genes. *PLoS One* 8: e57241.
- Van der Knaap MS, Smit LM, Barkhof F, Pijnenburg YA, Zweegman S et al. (2006). Neonatal porencephaly and adult stroke related to mutations in collagen IV A1. *Annals of Neurology* 59: 504-511.
- Wang Y, Sha N, Fang Y (2009). Analysis of genome-wide association data by large-scale Bayesian logistic regression. *BMC Proceedings* 3 Supplement 7: S16.
- Willour VL, Seifuddin F, Mahon PB, Jancic D, Pirooznia M et al. (2012). A genome-wide association study of attempted suicide. *Molecular Psychiatry* 17: 433-444.
- Wilson PM, Fryer RH, Fang Y, Hatten ME (2010). Astn2, a novel member of the astrotactin gene family, regulates the trafficking of ASTN1 during glial-guided neuronal migration. *Journal of Neuroscience* 30: 8529-8540.
- Yaramis A, Lochmüller H, Töpf A, Sonmezler E, Yilmaz E et al. (2020). COL4A1-related autosomal recessive encephalopathy in 2 Turkish children. *Neurology Genetics* 6: e392.
- Zhao JL, Li MH, Wang CL, Meng W (2016). A systematic review of Chiari I malformation: techniques and outcomes. *World Neurosurgery* 88: 7-14.

Supplementary data

Supplementary Table 1. Chromosomal variations in MTR family.

Index	Variation	Copy Number	Chromosome	Start	End	Lenght	Probe	Region
II-3	LOF	0	19	41381495	41381648	154	14	q13.2
II-3	LOF	0	19	41385334	41385869	536	12	q13.2
II-3	LOF	0	19	41386421	41386814	394	12	q13.2
II-3	LOF	0	22	24301392	24301824	433	15	q11.23
II-3	LOF	0	22	24302485	24302603	119	6	q11.23
II-3	LOF	0	22	42522134	42522313	180	7	q13.2
II-3	LOH	2	1	6145365	7613598	1468234	394	p36.31; p36.23
II-3	LOH	2	1	70257972	71841054	1583083	225	p31.1
II-3	LOH	2	1	93396819	94462243	1065425	187	p22.1
II-3	LOH	2	1	163508344	165825989	2317646	546	q23.3; q24.1
II-3	LOH	2	2	17822	1833668	1815847	495	p25.3
II-3	LOH	2	2	131112197	133040424	1928228	159	q21.1; q21.2
II-3	LOH	2	2	186224432	189857611	3633180	486	q32.1; q32.2
II-3	LOH	2	2	189859032	218663979	28804948	5881	q32.2; q32.3; q33.1; q33.2; q33.3; q34; q35
II-3	LOH	2	3	101232093	109465442	8233350	1462	q12.3; q13.11; q13.12; q13.13
II-3	LOH	2	3	186551711	188766239	2214529	705	q27.3; q28
II-3	LOH	2	5	17199259	27707936	10508678	1766	p15.1; p14.3; p14.2; p14.1
II-3	LOH	2	5	61758546	68829459	7070914	1181	q12.1; q12.2; q12.3; q13.1; q13.2
II-3	LOH	2	5	70398445	72911803	2513359	416	q13.2
II-3	LOH	2	7	152584806	159124173	6539368	2092	q36.1; q36.2; q36.3
II-3	LOH	2	13	106582808	115106996	8524189	2635	q33.2; q33.3; q34
II-3	LOH	2	14	38996493	40235485	1238993	179	q21.1
II-3	LOH	2	14	59214061	62979707	3765647	723	q23.1; q23.2
II-3	LOH	2	14	94579327	95678141	1098815	427	q32.12; q32.13
II-3	LOH	2	14	95684801	107283150	11598350	2811	q32.13; q32.2; q32.31; q32.32; q32.33
II-3	LOH	2	15	24008242	25907528	1899287	406	q11.2; q12
II-3	LOH	2	15	66372477	77276650	10904174	2552	q22.31; q22.32; q22.33; q23; q24.1; q24.2; q24.3
II-3	LOH	2	16	2133716	5180366	3046651	906	p13.3
II-3	LOH	2	16	22817446	27061619	4244174	1308	p12.2; p12.1
II-3	LOH	2	17	15647723	17200920	1553198	305	p12; p11.2
II-3	LOH	2	22	47105302	51214796	4109495	1515	q13.31; q13.32; q13.33
II-3	LOH	2	X	41302842	54735349	13432508	1963	p11.4; p11.3; p11.23; p11.22
II-3	LOH	2	X	107253323	108530481	1277159	126	q22.3
II-3	LOH	2	X	153363118	154913173	1550056	441	q28
II-3	LOH	2	X	88484868	89798620	1313753	193	q21.31
II-4	GOF	3	1	110230206	110241385	11180	72	p13.3
II-4	GOF	3	13	32914933	32915231	299	87	q13.1
II-4	LOF	0	19	41349596	41349656	61	9	q13.2
II-4	LOF	0	19	41381553	41381648	96	3	q13.2

Supplementary Table 1. Continued.

Index	Variation	Copy Number	Chromosome	Start	End	Lenght	Probe	Region
II-4	GOF	3	22	24374253	24385622	11370	119	q11.23
II-4	LOF	0	22	42522134	42522313	180	7	q13.2
II-4	LOH	2	1	6145365	7613598	1468234	394	p36.31; p36.23
II-4	LOH	2	1	163508344	165825989	2317646	546	q23.3; q24.1
II-4	LOH	2	1	190520424	191922512	1402089	196	q31.1; q31.2
II-4	LOH	2	2	4247903	7256134	3008232	731	p25.3; p25.2; p25.1
II-4	LOH	2	3	22204135	24882331	2678197	626	p24.3; p24.2
II-4	LOH	2	3	84961960	86378386	1416427	198	p12.1
II-4	LOH	2	3	101232093	122707286	21475194	4080	q12.3; q13.11; q13.12; q13.13; q13.2; q13.31; q13.32; q13.33; q21.1
II-4	LOH	2	4	38380620	40684941	2304322	569	p14
II-4	LOH	2	4	40686808	49620838	8934031	1556	p14; p13; p12; p11
II-4	LOH	2	4	52684820	55432159	2747340	467	q11; q12
II-4	LOH	2	4	180961974	182534983	1573010	482	q34.3
II-4	LOH	2	7	1604320	2911972	1307653	384	p22.3; p22.2
II-4	LOH	2	7	39423916	40485935	1062020	140	p14.1
II-4	LOH	2	8	172972	10464604	10291633	3729	p23.3; p23.2; p23.1
II-4	LOH	2	8	10480500	13002472	2521973	647	p23.1; p22
II-4	LOH	2	8	14020120	15045555	1025436	309	p22
II-4	LOH	2	8	23194680	43791691	20597012	4094	p21.3; p21.2; p21.1; p12; p11.23; p11.22 p11.21; p11.1
II-4	LOH	2	8	46936719	54991386	8054668	1202	q11.1; q11.21; q11.22; q11.23
II-4	LOH	2	9	25581774	45755225	20173452	2904	p21.3; p21.2; p21.1; p13.3; p13.2; p13.1; p12; p11.2
II-4	LOH	2	9	70906647	81587711	10681065	2205	q21.11; q21.12; q21.13; q21.2; q21.31
II-4	LOH	2	10	32054404	33708671	1654268	247	p11.22
II-4	LOH	2	11	84837883	86448092	1610210	272	q14.1; q14.2
II-4	LOH	2	13	106582808	111438085	4855278	1584	q33.2; q33.3; q34
II-4	LOH	2	15	24008242	25907528	1899287	406	q11.2; q12
II-4	LOH	2	16	24326722	27061619	2734898	689	p12.1
II-4	LOH	2	18	37617494	42358137	4740644	789	q12.3
II-4	LOH	2	20	1916836	4595025	2678190	754	p13
II-4	LOH	2	21	36528182	37981249	1453068	357	q22.12; q22.13
II-4	LOH	2	22	47105302	51214796	4109495	1515	q13.31; q13.32; q13.33
II-4	LOH	2	X	153363118	154913173	1550056	441	q28

Supplementary Table 2. Chromosomal variations in SOY family.

Index	Variation	Copy Number	Chromosome	Start	End	Lenght	Probe	Region
I-2	GOF	3	1	110220086	110245765	25680	85	p13.3
I-2	LOF	1	7	64693037	65087974	394938	43	q11.21
I-2	LOF	1	11	5248193	5248250	58	25	p15.4
I-2	GOF	3	11	37582575	38114401	531827	98	p12
I-2	LOF	0	19	41385334	41385775	442	9	q13.2
I-2	LOF	0	19	41386421	41386677	257	9	q13.2
I-2	LOF	0	22	42522134	42522313	180	7	q13.2
I-2	LOH	2	1	71051569	73583976	2532408	334	p31.1
I-2	LOH	2	3	28984225	50013778	21029554	5513	p24.1; p23; p22.3; p22.2; p22.1; p21.33; p21.32; p21.31
I-2	LOH	2	3	50129399	53662306	3532908	568	p21.31; p21.2; p21.1
I-2	LOH	2	4	8924210	10061147	1136938	155	p16.1
I-2	LOH	2	4	153882282	154995463	1113182	278	q31.3
I-2	LOH	2	5	63221842	64265857	1044016	131	q12.3
I-2	LOH	2	6	27339418	28641735	1302318	341	p22.1
I-2	LOH	2	7	86443168	87754969	1311802	373	q21.12
I-2	LOH	2	9	135425830	141068637	5642808	2342	q34.13 q34.2; q34.3
I-2	LOH	2	12	116775148	118395127	1619980	467	q24.21; q24.22; q24.23
I-2	LOH	2	13	111294811	112868642	1573832	492	q34
I-2	LOH	2	14	52006390	54290388	2283999	496	q22.1; q22.2
I-2	LOH	2	14	55997611	65701286	9703676	2108	q22.3; q23.1; q23.2; q23.3
I-2	LOH	2	15	43818532	45440621	1622090	300	q15.3; q21.1
I-2	LOH	2	16	3370894	6896128	3525235	1231	p13.3
I-2	LOH	2	17	13671552	22234751	8563200	1690	p12 p11.2; p11.1
I-2	LOH	2	17	25311244	31320695	6009452	1060	q11.1; q11.2
I-2	LOH	2	19	41928183	59097933	17169751	5017	q13.2; q13.31; q13.32; q13.33; q13.41; q13.42; q13.43
I-2	LOH	2	21	25902463	39947747	14045285	3245	q21.2; q21.3; q22.11; q22.12; q22.13; q22.2
I-2	LOH	2	22	31535872	32662384	1126513	185	q12.2; q12.3
I-2	LOH	2	22	45395342	49074301	3678960	1247	q13.31; q13.32
I-2	LOH	2	22	49591992	51214796	1622805	626	q13.33
I-2	LOH	2	X	86683205	87698139	1014935	225	q21.31
II-2	GOF	3	1	110228436	110245765	17330	84	p13.3
II-2	LOF	1	11	5248193	5248250	58	25	p15.4
II-2	LOF	1	16	30208520	30212911	4392	29	p11.2
II-2	LOF	1	19	11224269	11224319	51	16	p13.2
II-2	LOF	1	19	11231099	11231159	61	23	p13.2
II-2	LOF	1	19	41381495	41381648	154	14	q13.2
II-2	LOF	0	19	41382010	41382256	247	3	q13.2
II-2	LOF	1	19	41384103	41385869	1767	39	q13.2
II-2	LOF	0	22	24301392	24301695	304	12	q11.23
II-2	LOF	1	22	24301824	24302487	664	24	q11.23

Supplementary Table 2. Continued.

Index	Variation	Copy Number	Chromosome	Start	End	Lenght	Probe	Region
II-2	GOF	3	22	24375632	24385472	9841	102	q11.23
II-2	LOF	0	22	42522134	42522397	264	10	q13.2
II-2	GOF	2	X	48303837	48386632	82796	39	p11.23
II-2	GOF	2	X	99661925	99663226	1302	31	q22.1
II-2	LOF	0	Y	2654333	10068588	7414256	1564	p11.31; p11.2
II-2	LOF	0	Y	13133499	19567718	6434220	2157	q11.1; q11.21; q11.221
II-2	LOF	0	Y	20804835	24522333	3717499	1197	q11.222; q11.223
II-2	LOF	0	Y	28509482	28817636	308155	32	q11.23; q12
II-2	LOH	2	1	54124121	68741305	14617185	3487	p32.3; p32.2; p32.1; p31.3
II-2	LOH	2	1	118941488	120405606	1464119	290	p12
II-2	LOH	2	2	40078780	47639559	7560780	2169	p22.1; p21
II-2	LOH	2	2	47639598	49190917	1551320	1207	p21; p16.3
II-2	LOH	2	2	49194702	51819167	2624466	582	p16.3
II-2	LOH	2	3	417207	3518222	3101016	1023	p26.3; p26.2
II-2	LOH	2	3	3526289	16281960	12755672	4051	p26.2; p26.1; p25.3; p25.2; p25.1
II-2	LOH	2	3	53599972	60113719	6513748	1523	p21.1; p14.3; p14.2
II-2	LOH	2	4	8924210	10416360	1492151	241	p16.1
II-2	LOH	2	4	76475804	84664343	8188540	1570	q21.1; q21.21; q21.22; q21.23
II-2	LOH	2	4	121814232	124359046	2544815	504	q27; q28.1
II-2	LOH	2	4	154938646	163486514	8547869	1766	q31.3; q32.1; q32.2
II-2	LOH	2	4	174490092	176125249	1635158	366	q34.1
II-2	LOH	2	5	88215821	90698051	2482231	478	q14.3
II-2	LOH	2	6	162699	6780870	6618172	1943	p25.3; p25.2; p25.1
II-2	LOH	2	6	27339418	28470909	1131492	303	p22.1
II-2	LOH	2	7	134976271	151415504	16439234	4120	q33; q34; q35; q36.1
II-2	LOH	2	8	73231464	92409428	19177965	3207	q13.3; q21.11; q21.12; q21.13; q21.2; q21.3
II-2	LOH	2	8	92419127	112996602	20577476	3869	q21.3; q22.1; q22.2; q22.3; q23.1; q23.2; q23.3
II-2	LOH	2	9	4355828	7231323	2875496	751	p24.2; p24.1
II-2	LOH	2	9	87666681	94821398	7154718	1568	q21.33; q22.1; q22.2; q22.31
II-2	LOH	2	9	95700701	105041325	9340625	1947	q22.31; q22.32; q22.33; q31.1
II-2	LOH	2	9	135284962	136411084	1126123	582	q34.13; q34.2
II-2	LOH	2	9	136414531	140377226	3962696	1654	q34.2; q34.3
II-2	LOH	2	10	82704505	90740501	8035997	1817	q23.1; q23.2; q23.31
II-2	LOH	2	10	105721994	117935672	12213679	2482	q24.33; q25.1; q25.2; q25.3
II-2	LOH	2	10	118201081	120767115	2566035	680	q25.3; q26.11
II-2	LOH	2	11	71287843	84543955	13256113	2912	q13.4; q13.5; q14.1
II-2	LOH	2	11	84545984	85993211	1447228	219	q14.1; q14.2
II-2	LOH	2	11	86040620	94708891	8668272	1742	q14.2; q14.3; q21
II-2	LOH	2	11	114074756	120678788	6604033	1893	q23.2; q23.3
II-2	LOH	2	12	74028301	75054053	1025753	124	q21.1

Supplementary Table 2. Continued.

Index	Variation	Copy Number	Chromosome	Start	End	Lenght	Probe	Region
II-2	LOH	2	12	106729425	118395127	11665703	2819	q23.3; q24.11; q24.12; q24.13; q24.21; q24.22; q24.23
II-2	LOH	2	12	129107131	132104045	2996915	1127	q24.32; q24.33
II-2	LOH	2	12	132124118	133801770	1677653	437	q24.33
II-2	LOH	2	15	40725601	41829178	1103578	208	q15.1
II-2	LOH	2	15	98720899	100928615	2207717	732	q26.3
II-2	LOH	2	16	92688	4417797	4325110	1683	p13.3
II-2	LOH	2	16	84314573	85915218	1600646	657	q24.1
II-2	LOH	2	17	26800204	27889643	1089440	196	q11.2
II-2	LOH	2	18	30089478	43049523	12960046	2186	q12.1; q12.2; q12.3
II-2	LOH	2	18	43065107	44181227	1116121	352	q12.3; q21.1
II-2	LOH	2	18	55839162	59015339	3176178	832	q21.31; q21.32; q21.33
II-2	LOH	2	18	59020751	70724185	11703435	2705	q21.33; q22.1; q22.2; q22.3
II-2	LOH	2	20	19885390	26266524	6381135	1189	p11.23; p11.22; p11.21; p11.1
II-2	LOH	2	20	29459599	36296688	6837090	1092	q11.21; q11.22; q11.23
II-2	LOH	2	20	36305516	39043958	2738443	525	q11.23; q12
II-2	LOH	2	20	39045734	40070246	1024513	238	q12
II-2	LOH	2	20	40078085	55450089	15372005	3982	q12; q13.11; q13.12; q13.13; q13.2; q13.31
II-2	LOH	2	21	18457828	21038473	2580646	613	q21.1
II-2	LOH	2	21	25902463	36223627	10321165	2267	q21.2; q21.3; q22.11; q22.12
II-2	LOH	2	X	519500	1846919	1327420	228	p22.33

GOF: gain of function, LOH: loss of heterozygosity, LOF: loss of function.